A&A 558, L6 (2013)
DOI: 10.1051/0004-6361/201322201

Astronomy & Astrophysics

Letter to the Editor

SOPHIE velocimetry of *Kepler* transit candidates

IX. KOI-415 b: a long-period, eccentric transiting brown dwarf to an evolved Sun⋆,⋆⋆

C. Moutou[1], A. S. Bonomo[2], G. Bruno[1], G. Montagnier[3,4], F. Bouchy[1], J. M. Almenara[1], S. C. C. Barros[1], M. Deleuil[1], R. F. Díaz[1], G. Hébrard[3,4], and A. Santerne[5]

[1] Aix Marseille Université, CNRS, LAM (Laboratoire d'Astrophysique de Marseille) UMR 7326, 13388 Marseille, France
e-mail: Claire.Moutou@oamp.fr
[2] INAF – Osservatorio Astrofisico di Torino, via Osservatorio 20, 10025, Pino Torinese, Italy
[3] Institut d'Astrophysique de Paris, UMR 7095 CNRS, Université Pierre & Marie Curie, 98bis boulevard Arago, 75014 Paris, France
[4] Observatoire de Haute-Provence, CNRS/OAMP, 04870 Saint-Michel-l'Observatoire, France
[5] Centro de Astrofísica, Universidade do Porto, Rua das Estrelas, 4150-762 Porto, Portugal

Received 3 July 2013 / Accepted 23 August 2013

ABSTRACT

We report the discovery of a long-period brown-dwarf transiting companion of the solar-type star KOI-415. The transits were detected by the *Kepler* space telescope. We conducted Doppler measurements using the SOPHIE spectrograph at the Observatoire de Haute-Provence. The photometric and spectroscopic signals allow us to characterize a 62.14 ± 2.69 $M_{\rm Jup}$ brown-dwarf companion of an evolved 0.94 ± 0.06 $M_{\odot}$ star in a highly eccentric orbit of P = 166.78805 ± 0.00022 days and e = 0.698 ± 0.002. The radius of KOI-415 b is $0.79^{+0.12}_{-0.07}$ $R_{\rm Jup}$, a value that is compatible with theoretical predictions for a 10 Gyr, low-metallicity and non-irradiated object.

Key words. planetary systems – techniques: photometric – techniques: spectroscopic – techniques: radial velocities – stars: brown dwarfs – stars: individual: KIC6289650

1. Introduction

Transiting brown dwarfs (BD) are much less common than transiting giant planets. Above 20 $M_{\rm Jup}$, only eight such objects are known: CoRoT-3 b (Deleuil et al., 2008), KELT-1 b (Siverd et al., 2012), KOI-205 b (Díaz et al., 2013), the young pair of eclipsing brown dwarfs 2M0535-05 (Stassun et al., 2007), WASP-30 b (Triaud et al., 2013), LHS 6343 C (Johnson et al., 2011), and CoRoT-15 b (Bouchy et al., 2011). The precise measurement of their mass and radius offers important constraints for the transition region between giant planets and low-mass stars, to be compared with theoretical predictions as given by, for instance, Burrows et al. (1997), Chabrier et al. (2000) and Baraffe et al. (2003). If CoRoT-15 b appears to be inflated, WASP-30 b, LHS 6343 C and KOI-205 b have a radius compatible with their age, as predicted by models. 2M0535-05 A and B may have smaller radii than predicted because of their activity (Stassun et al., 2012).

In this paper, we report the discovery and characterization of a new transiting brown dwarf in a long-period and highly-eccentric orbit: KOI-415 b is one the ∼2300 transiting candidates identified by *Kepler* (Batalha et al., 2013). The host star is a 14.11 magnitude star identified as KIC 6289650 or 2MASS-19331345+4136229. The transiting companion has been established as a brown dwarf by complementary observations with the SOPHIE radial-velocity instrument. KOI-415 b is one of the few known *Kepler* objects of interest (KOI) that lie in the brown dwarf domain and not in the planet domain (as KOI-205 b), a type of false-positive scenario whose low-occurrence is favored by the "brown-dwarf desert", however.

2. Data

2.1. Kepler photometry

KOI-415 was observed by *Kepler* with a temporal sampling of 29.4 min (long-cadence data) for 1239.8 days; short-cadence data (one point per minute) are not available for this target. The ∼59 000 raw simple-aperture-photometry measurements, which cover fourteen quarters, from Q1 to Q14, were downloaded from the MAST archive[1]. The flux excess caused by background stars that contaminate the photometric mask, as estimated by the *Kepler* team for each quarter[2], does not exceed 5% of the total flux collected by *Kepler* and was subtracted from the raw data.

The light curve exhibits seven transits with a period of 166.8 d, a depth of ∼0.5%, and a duration of ∼6 h. The median of the errors of the individual measurements is 185 ppm. Figure 1 displays the phase-folded transit of KOI-415 b.

No variations attributable to starspots and faculae on the stellar photosphere are noticed, which indicates that the star is magnetically quiet.

⋆ Based on observations collected with the NASA *Kepler* satellite and with the SOPHIE spectrograph on the 1.93-m telescope at Observatoire de Haute-Provence (CNRS), France.
⋆⋆ Table 1 is available in electronic form at http://www.aanda.org

[1] http://archive.stsci.edu/kepler/data_search/search.php
[2] http://archive.stsci.edu/kepler/kepler_fov/search.php

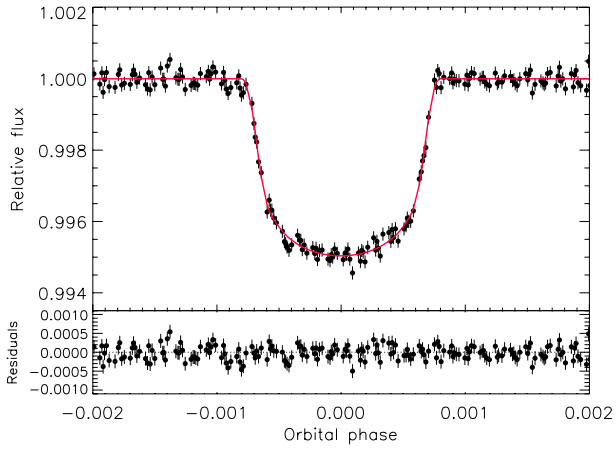

Fig. 1. *Top panel*: phase-folded transit light curve of KOI-415. The red solid line shows the transit model rebinned at the *Kepler* sampling rate (see text for explanation). *Bottom panel*: residuals between the observations and the best-fit model.

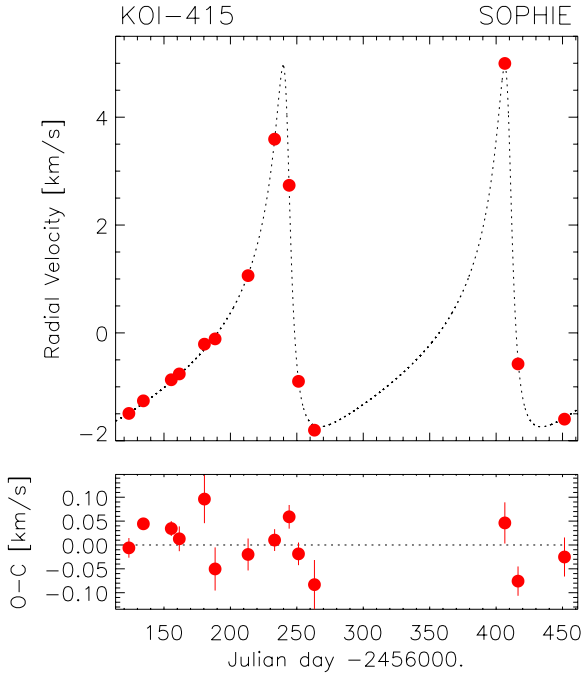

Fig. 2. Radial velocities of KOI-415 obtained by SOPHIE as a function of time. The bottom plot shows the residuals after subtracting the model.

2.2. SOPHIE spectroscopy and velocimetry

We have secured 14 measurements of KOI-415 from July 2012 to June 2013 with the SOPHIE spectrograph at Observatoire de Haute-Provence. SOPHIE is an echelle optical spectrograph in a thermally controlled room, fed by a fiber link from the Coudé focus of the 1.93-m telescope. It covers the range 390–687 nm at a resolving power of 40 000 in high-efficiency (HE) mode; the acceptance on the sky is 3″ diameter. The radial velocities (RV) were extracted with the SOPHIE pipeline by measuring the cross-correlation function (CCF) of the spectra with a numerical mask of a G2 star, following the method described in Baranne et al. (1996). The CCF was measured without the seven bluest orders, which are dominated by noise. The G2 mask is preferred above the other F0 and K5 masks because it gives lower-noise measurements. The average RV uncertainty of the 14 measurements of KOI-415 is 31 m s^{-1}.

When the background was bright, the CCF in the neighboring sky fiber was subtracted from the stellar CCF before the stellar CCF was fitted by a Gaussian model. In four spectra out of the 14, the background was detected and the RV were corrected for the contamination, with offsets varying from 13 m s^{-1} to 100 m s^{-1}. The final measurements are listed in Table 1 together with the exposure time, signal-to-noise ratio (S/N) per spectrum, and the bisector span of the CCF.

The radial velocities exhibit a scatter of 2 km s^{-1}. Their variations are in phase with the *Kepler* photometric transit event and compatible with the highly eccentric orbit of a massive object, as plotted in Fig. 2.

The bisector spans were used to check that the stellar CCF was not blended by an additional stellar spectrum, as is commonly done in transit-validation processes (Torres et al, 2004; Bouchy et al., 2009). The bisector spans of KOI-415 do not vary significantly in our data set, and show a dispersion of 75 ± 60 m s^{-1}.

3. Host star

After RV corrections, all spectra that were only weakly affected by the moon reflected light were co-added. This resulted in a final spectrum with a S/N of 120 per pixel at 5500 Å. The effective temperature $T_{\rm eff}$, surface gravity $\log g$, and metallicity [Fe/H] were estimated by using the versatile wavelength analysis package (VWA; Bruntt et al. 2004, 2010). We selected 242 spectral lines of FeI and FeII and fitted them iteratively, until the derived abundances minimized the correlation with the respective equivalent width and excitation potential and the mean FeI and FeII abundances coincided. $v_{\rm macro}$ was fixed according to $T_{\rm eff}$ following Bruntt et al. (2010) to the value 2.4 km s^{-1}. $v_{\rm micro}$ was fixed to 1.6 km s^{-1}.

KOI-415 appears to be a slightly evolved solar-type star with $T_{\rm eff}$ = 5810 ± 80 K, $\log g$ = 4.5 ± 0.2 and [Fe/H] = −0.24 ± 0.11. We derived $\log g$ from the pressure-sensitive lines of Ca at 6122, 6162 and 6439 Å and from the MgIb line at 5172 Å, as well. The best fit was obtained from the Ca6122 and the Ca6162 lines (4.34 ± 0.26 dex) and agrees with the result from the Fe lines. Abundances of elements presenting isolated lines were calculated. Using an estimated $B - V$ value of 0.58, the CCF parameters correspond to a projected rotational velocity of 2.8 ± 1.5 km s^{-1}. The spectroscopic $v \sin i$ was derived by fitting a set of isolated spectral lines to the corresponding synthetic profiles, which were convolved with different rotational profiles. Its low value (1 ± 1 km s^{-1}) is compatible within 1.2σ with the CCF estimate. The low $v \sin i$ confirms the hypothesis that KOI-415 is an evolved star. Furthermore, no activity was observed through the CaII H and K lines. Using the spectroscopically determined $v \sin i$ and the stellar radius, the projected spin period of the star is 30 to 60 days. The final parameters of the host star are derived after the transit modeling in the next section.

4. Modeling the data and parameter estimation

Before starting the combined analysis of *Kepler* and SOPHIE data, a preliminary fit of the radial-velocity data was performed with a Keplerian model by using the downhill simplex algorithm (Press et al., 1992) and fixing the transit epoch and the orbital period to the values determined from the photometry. From the best solution, the uncertainties of SOPHIE data were scaled to derive a reduced $\chi^2 = 1$. The scaling factor corresponds to an RV jitter of 39 m s^{-1}.

The transits were normalized by locally fitting a parabola to the 10 h intervals of the light curve before the ingress and after the egress of each transit. The seventh transit, which occured at 2456078.870 BJD_{TBD}, was not considered for our analysis because a gap taking place before its ingress prevented us from properly normalizing it. Photometrically correlated noise was estimated following Pont et al. (2006) and Bonomo et al. (2012), but its contribution was found to be negligible.

The eleven free parameters of our combined fit are the transit epoch T_0, the orbital period P, the systemic RV V_r, the RV semi-amplitude K, $\sqrt{e}\cos\omega$ and $\sqrt{e}\sin\omega$, where e is the eccentricity and ω the argument of periastron, the transit duration T_{14}, the ratio of the brown dwarf to stellar radii R_b/R_*, the inclination i between the orbital plane and the plane of the sky, and the two limb-darkening coefficients $u_+ = u_a + u_b$ and $u_- = u_a - u_b$.

The transit fitting was carried out using the model of Giménez (2006, 2009) and a denser temporal sampling $\delta t_{model} = \delta t/5$, to overcome the problem of the coarse long-cadence sampling that distorts the transit shape (Kipping, 2010). The χ^2 of each trial model was then computed by binning the model samples at the *Kepler* sampling rate δt. An initial combined fit was performed by using the algorithm AMOEBA (Press et al., 1992) and changing the initial values of the parameters with a Monte Carlo method to properly explore the parameter space.

The posterior distributions of our free parameters were determined by means of a differential evolution Markov chain Monte Carlo (DE-MCMC) method which is an MCMC version of the genetic algorithm (Ter Braak, 2006; Eastman et al., 2013). Twenty-two chains, which is twice the number of the fitted parameters, were simultaneously run after starting at different positions in the parameter space but reasonably close to the best solution previously found with AMOEBA. The jumps for a current chain in the parameter space were determined from the other chains according to the prescriptions given by Ter Braak (2006).The Metropolis-Hastings algorithm was used to accept or reject a proposal step for each chain. Uniform priors were implicitly imposed for all parameters except for the limb-darkening coefficients, for which Gaussian priors were considered, that is, $N_{u_+}(0.7, 0.07)$ and $N_{u_-}(0.15, 0.14)$, where the most probable values were determined by the exploratory fit with AMOEBA.

Our DE-MCMC stopped when the convergence of the chains was achieved according to Ford (2006), that is, when the Gelman-Rubin statistics was lower than 1.01 (Gelman et al., 2004) and the number of independent draws was greater than 1000. Steps belonging to the "burn-in" phase, which were identified following Knutson et al. (2009) and Eastman et al. (2013), were discarded.

The medians of the posterior distributions of the fitted and derived parameters and their 34% intervals are quoted in Table 2 as the final values and their 1σ uncertainties, respectively.

The RV observations carried out with SOPHIE and the solution of the Keplerian fit derived from our combined fit are shown in Fig. 2. The scatter of the residuals is 71 m/s. Figure 1 displays the phase-folded transit of KOI-415 b and the transit model. The photometric residuals show an rms of 177 ppm, consistent with the median error of the data points (185 ppm). The rms over 3 h is 72 ppm, in agreement with the combined differential photometric precision of ~85 ppm (Gilliland et al., 2011) provided by the *Kepler* team.

The stellar density derived from the transit fitting and the Yonsey-Yale evolutionary tracks (Demarque et al., 2004) for the effective temperature and metallicity of KOI-415 indicate that with a mass $M_\star = 0.94 \pm 0.06\ M_\odot$, a radius $R_\star = 1.25^{+0.15}_{-0.10}\ R_\odot$, and age of 10.5 ± 2.2 Gyr at 1σ, this star is slightly evolved. This is compatible with the absence of activity-related features in the *Kepler* light curve. The photometric $\log g = 4.22^{+0.06}_{-0.09}$ dex agrees with the spectroscopic value, which is more uncertain.

Table 2. KOI-415 system parameters.

Fitted system parameters	
BD orbital period P [days]	166.78805 ± 0.00022
BD transit epoch T_0[$BJD_{TDB} - 2454900$]	178.14187 ± 0.00063
BD transit duration T_{14} [h]	$6.01^{+0.11}_{-0.07}$
Radius ratio R_p/R_*	$0.0649^{+0.0017}_{-0.0013}$
Inclination i [deg]	$89.31^{+0.40}_{-0.38}$
Limb-darkening coefficient u_+	0.70 ± 0.05
Limb-darkening coefficient u_-	0.13 ± 0.12
$\sqrt{e}\cos\omega$	0.592 ± 0.005
$\sqrt{e}\sin\omega$	0.590 ± 0.005
Radial velocity semi-amplitude K [km s^{-1}]	3.346 ± 0.021
Systemic velocity V_r [km s^{-1}]	-1.492 ± 0.011
Derived orbital parameters	
Orbital eccentricity e	0.698 ± 0.002
Argument of periastron ω [deg]	44.9 ± 0.6
Derived transit parameters	
a/R_*	$100.0^{+7.5}_{-10.1}$
Stellar density ρ_* [g cm^{-3}]	$0.68^{+0.16}_{-0.18}$
Impact parameter b	$0.41^{+0.16}_{-0.23}$
Limb-darkening coefficient u_a	0.42 ± 0.05
Limb-darkening coefficient u_b	0.28 ± 0.07
Atmospheric parameters of the star	
Effective temperature T_{eff}[K]	5810 ± 80
Spectroscopic surface gravity $\log g$ [cgs]	4.5 ± 0.2
Photometric surface gravity $\log g$ [cgs]	$4.22^{+0.06}_{-0.09}$
Metallicity [Fe/H] [dex]	-0.24 ± 0.11
Stellar rotational velocity $V \sin i_*$ [km s^{-1}]	1.0 ± 1
Spectral type	G0IV
Star and companion physical parameters	
Stellar mass [$M_\odot$]	0.94 ± 0.06
Stellar radius [$R_\odot$]	$1.25^{+0.15}_{-0.10}$
BD mass M_b [M_{Jup}]	62.14 ± 2.69
BD radius R_b [R_{Jup}]	$0.79^{+0.12}_{-0.07}$
BD density ρ_b [g cm^{-3}]	$157.4^{+51.4}_{-52.3}$
BD surface gravity $\log g_b$ [cgs]	$5.39^{+0.08}_{-0.11}$
Age t [Gyr]	10.5 ± 2.2
Orbital semi-major axis a [AU]	0.593 ± 0.013
Orbital distance at periastron a_{per} [AU]	0.179 ± 0.004
Orbital distance at apastron a_{apo} [AU]	1.006 ± 0.021

The derived coefficients of the quadratic limb-darkening law $u_a = 0.42 \pm 0.05$ and $u_b = 0.28 \pm 0.07$ agree very well with the values determined by Sing (2010) using Kurucz stellar models (Kurucz, 1993) and the *Kepler* bandpass[3], after linearly interpolating at the T_{eff}, $\log g$ and metallicity of the star, that is, $u_a = 0.36 \pm 0.02$ and $u_b = 0.28 \pm 0.01$.

According to the determined stellar parameters, the mass and radius of the brown dwarf KOI-415 b are $M_b = 62.14 \pm 2.69\ M_{Jup}$ and $R_b = 0.79^{+0.12}_{-0.07}\ R_{Jup}$. The corresponding density is $157.4^{+51.4}_{-52.3}$ g cm^{-3}. Its very large error is dominated by the uncertainty on the brown dwarf radius.

[3] http://vega.lpl.arizona.edu/singd/David_Sing/Limb_Darkening.html

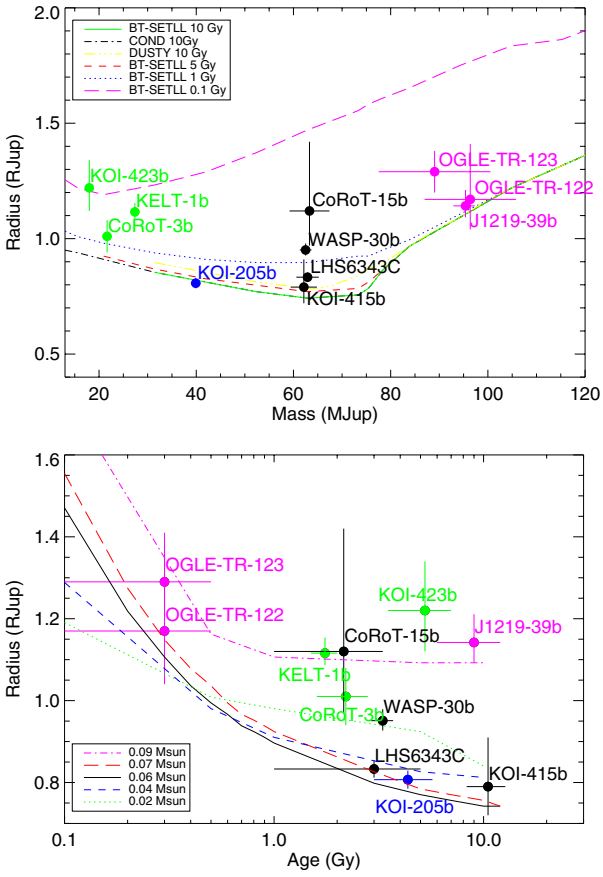

Fig. 3. *Top panel*: mass-radius diagram in the transition domain between brown dwarfs and stars. Isochrones for 10, 5, 1, and 0.1 Gyr are shown for comparison. *Bottom panel*: radius as a function of system's age for objects from 15 to 100 Jupiter masses. BT-SETTL isochrones are shown for 0.02 to 0.09 $M_{\odot}$. Color symbols indicate the mass range: 15–25 $M_{\rm Jup}$ (green), 37–40 $M_{\rm Jup}$ (blue), 59–65 $M_{\rm Jup}$ (black), and 89–97 $M_{\rm Jup}$ (pink).

5. Discussion

Figure 3 (top) shows the mass and radius of KOI-415 b and other similar objects in the transition domain between giant planets and low-mass stars. They are compared with values predicted by isochrones[4] for models of isolated BDs developed by Chabrier et al. (2000), Allard et al. (2001), and Baraffe et al. (2003). With its long period (166.8 days), KOI-415 b more closely resembles the isolated BD as modeled in the tracks than the short-period companions more easily found by transiting surveys. The radius of KOI-415 b perfectly fits the predicted radius for a system age of 10 Gy and a non-metallic system with a cloud-free atmosphere (Burrows et al., 1997; Baraffe et al., 2003; Burrows et al., 2011). It shows that long-period BDs are adequately supported by partial electron degeneracy physics with a quantitatively correct equation of state. Brown dwarfs such as KOI-415 b are among the smallest ones in size, corresponding to the evolved state of its system, its low metallicity and low irradiation. It is also the oldest characterized BD (Fig. 3 (bottom)).

The models predict an effective temperature of 950 K for KOI-415 b. With an eccentricity of about 0.7 and period of 166.8 days, the temperature of the dayside of the brown dwarf likely increases by as much as 400 K along its orbit, from periastron to apastron due to changing stellar irradiation. It could be interesting to investigate, with dedicated modeling, the impact on the internal structure this seasonal effect may have.

Finally, the speckle imaging of the field around KOI-415 shows the existence of a nearby companion with a magnitude difference 2.9 in the optical, at 1.93″ from the main target[5]. If it were bound to the main star, this companion would be an M1 dwarf at about 1600 AU orbital distance. The existence of such a stellar companion could then explain the high eccentricity of the brown dwarf KOI-415 b. Doppler measurements collected over a few years timescale could be sufficient to unveil their relationship; a background star is also a possibility.

Acknowledgements. A.S.B. gratefully acknowledges support through INAF/HARPS-N fellowship. We thank the staff at Haute-Provence Observatory. We acknowledge the PNP of CNRS/INSU, and the French ANR for their support. R.F.D. is supported by CNES. AS acknowledges the support by the European Research Council/European Community under the FP7 through Starting Grant agreement number 239953.

References

Allard, F., Hautschild, P. H., Alexander, D. R., et al. 2001, ApJ, 556, 357
Baraffe, I., Chabrier, G., Barman, T., et al. 2003, A&A, 402, 701
Baranne, A., Queloz, D., Mayor, M., et al. 1996, A&AS, 119, 373
Batalha, N., Rowe, J. F., Bryson, S. T., et al. 2013, ApJS, 204, 24
Bonomo, A., S., Chabaud, P. Y., Deleuil, M., et al. 2012, A&A, 547, A110
Bouchy, F., Moutou, C., & Queloz, D. 2009, IAU, 253, 129
Bouchy, F., Deleuil, M., Guillot, T., et al. 2011, A&A, 525, A68
Bruntt, H., Bikmaev, I. F., Catala, C., et al. 2004, A&A, 425, 683
Bruntt, H., Bedding, T., Quirion, P., et al. 2010, MNRAS, 405, 1907
Burrows, A., Marley, M., Hubbard, W. B., et al. 1997, ApJ, 491, 856
Burrows, A., Heng, K. & Nampaisarn, T. 2011, ApJ, 736, 47
Chabrier, G., Baraffe, I., Allard, F., & Hauschildt, P. 2000, ApJ, 542, 464
Deleuil, M., Deeg, H., Alonso, R., et al. 2008, A&A, 49, 889
Demarque, Woo, & Kim, Yi 2004, ApJS, 155, 667
Díaz, R. F., Damiani, C., Deleuil, M., et al. 2013, A&A 551, L9
Eastman, J., Siverd, R., & Gaudi, B. S. 2010, PASP, 122, 935
Eastman, J., Gaudi, B. S., & Agol, E. 2013, PASP, 125, 923
Ford, E. B. 2006, ApJ, 642, 505
Gelman, A., Carlin, J. B., Steen, H. S., et al. 2004, Bayesian data analysis (Chapman & Hall)
Gilliland, R., Chaplin, W., Dunham, E., et al. 2011, ApJS, 197, 6
Giménez, A. 2006, A&A, 450, 1231
Giménez, A. 2009, ASP, 450, 291
Johnson, J. A., Apps, K., Gazak, J. Z., et al. 2011, ApJ, 730, 79
Kipping, D. 2010, MNRAS, 408, 1758
Knutson, H., Charbonneau, D., Cowan, N., et al. 2009, ApJ, 703, 769
Kurucz, R. I. 1993, ATLAS9 Stellar Atmosphere Programs (Cambridge, Mass: Smithsonian Astrophysical observatory)
Pont, F., Zucker, S., & Queloz, D. 2006, MNRAS, 373, 231
Press, W. H., Teukolsky, S. A., Vetterling, W. T. 1992, Numerical recipes in FORTRAN, 2nd edn. (Cambridge: University press)
Sing, D. K. 2010, A&A, 510, A21
Siverd, R. J., Beatty, T. G., Pepper, J., et al. 2012, ApJ, 761, 123
Stassun, K. G., Mathieu, R. D., & Valenti, J. A. 2007, ApJ, 664, 1154
Stassun, K., Kratter, K., Scholz, A., & Dupuy, T. 2012, ApJ, 756, 47
Ter Braak, C. J. F. 2006, Statistics and Computing, 16, 239
Torres, G., Konacki, M., Sasselov, D. D., & Jha, S. 2004, ApJ, 614, 979
Triaud, A. H. M. J., Hebb, L., Anderson, A., et al. 2013, A&A, 549, A18

[4] http://phoenix.ens-lyon.fr/Grids

[5] https://cfop.ipac.caltech.edu/

Table 1. Radial velocity measurements for KOI-415.

BJD_{UTC} –2 456 000	RV (km s^{-1})	σ_{RV} (km s^{-1})	Bis (km s^{-1})	T_{exp} (s)	S/N / pix (550 nm)
123.5860	–2.903	0.021	–0.052	2700	14
134.4912	–2.669	0.012	–0.006	3600	22
155.4896	–2.279	0.016	0.021	3600	19
161.5256	–2.169	0.027	0.011	1521	13
180.4504	–1.594	0.052	–0.116	900	10
188.4825	–1.533	0.047	0.141	900	9
213.3051	–0.349	0.034	–0.103	1940	13
233.2643	2.172*	0.024	0.038	1800	16
244.2319	1.371*	0.032	–0.097	1210	12
251.2602	–2.313*	0.024	0.027	1800	16
263.2605	–3.181	0.054	0.074	1800	10
406.5797	3.569*	0.046	0.0013	2700	10
416.5095	–1.985	0.031	0.052	1503	14
451.4736	–2.987	0.041	0.046	2202	11

Notes. Asterisks show the measurements corrected for the background light.